

---

<https://doi.org/10.15407/ujpe68.3.184>

R.K. JHAKAL,<sup>1</sup> M.D. SHARMA,<sup>1</sup> U. PALIWAL<sup>2</sup>

<sup>1</sup> Department of Physics, Government Dungar College  
(Bikaner-334001, India; e-mail: sharmamd.physics@gmail.com)

<sup>2</sup> Department of Physics, Jai Narain Vyas University  
(Jodhpur-342001, India)

## A THEORETICAL ESTIMATION OF OPTICAL, VIBRATIONAL AND STRUCTURAL PROPERTIES OF II–VI QUATERNARY ALLOY $Zn_{0.5}Cd_{0.5}S_ySe_{1-y}$

---

We present a theoretical estimation of optical, vibrational, and structural properties of II–VI semiconducting quaternary alloy  $Zn_{0.5}Cd_{0.5}S_ySe_{1-y}$  for  $0 < y < 1$  giving total 10 compositions. The estimation of refractive index, elastic constants, bulk modulus, and vibrational frequencies are performed using the important input parameters provided by the empirical pseudopotential method. In this method, the bandgaps are computed, and the alloying effects are modeled through the modified virtual crystal approximation. We have computed the static refractive index, static and high-frequency dielectric constants, longitudinal and transverse optical phonon frequencies, elastic constants, bulk modulus, and cohesive energy for 10 compositions of the alloy. The results are compared to other experimental and theoretical values wherever available.

*Keywords:* II–VI quaternary alloys, empirical pseudopotential method, elastic constants.

### 1. Introduction

The II–VI semiconducting compounds are composed of metal atoms of IIB group (Zn, Cd, Hg, etc.) and VIA group anions (O, S, Se, Te). These materials generally crystallize in cubic zinc-blende or wurtzite type structures. The bonding in the II–VI materials has ionic character, so that the materials show larger bandgaps than those for III–V and other semiconductors. Thus, these materials are also known as wide-bandgap semiconductors. Due to a large value of bandgap ( $E_g > 2$  eV), the device based on these

materials will show a shorter emission/absorption wavelength in the blue-green and UV regions. The bandgap and lattice properties of II–VI materials can be tuned easily by making the II–VI ternary and quaternary alloys. These alloys open up a new era of opto-electronic devices of desired bandgaps and absorption spectra. One can tune the bandgap and other properties easily by altering the composition in the ternary and quaternary alloys. A very important advantage of II–VI ternary and quaternary alloys is their lattice matching with III–V semiconductors, which makes it possible to grow the thin films of these materials on substrate like GaAs, InP, etc. Another big advantage of II–VI materials is the large life time of opto-electronic devices based on them. Due to these features, the II–VI ternary and quaternary semiconducting alloys have extensive applications in light emitting diodes, laser diodes, photoelectrochemical cells, photo-transistors, photorefrac-

---

Citation: Jhokal R.K., Sharma M.D., Paliwal U. A theoretical estimation of optical, vibrational and structural properties of II–VI quaternary alloy  $Zn_{0.5}Cd_{0.5}S_ySe_{1-y}$ . *Ukr. J. Phys.* **68**, No. 3, 184 (2023). <https://doi.org/10.15407/ujpe68.3.184>.  
Цитування: Джакал Р.К., Шарма М.Д., Палівал Ю. Теоретична оцінка оптичних, вібраційних та структурних властивостей сплаву з елементами II та VI груп  $Zn_{0.5}Cd_{0.5}S_ySe_{1-y}$ . *Укр. фіз. журн.* **68**, № 3, 184 (2023).

tive materials, thin-film-based solar cells, electro-modulation devices, photoconductive sensors, and electroluminescent devices [1–14].

The  $\text{Zn}_x\text{Cd}_{1-x}\text{S}_y\text{Se}_{1-y}$  quaternary alloy is an important member of II–VI materials. It is experimentally fabricated on GaAs and InP and shows useful applications in various optoelectronic devices [15, 16]. In this paper, we present the computed optical, vibraional, and structural parameters for 10 compositions of  $\text{Zn}_{0.5}\text{Cd}_{0.5}\text{S}_y\text{Se}_{1-y}$  II–VI semiconducting quaternary alloy. The refractive index, and static and high-frequency dielectric constants are computed to understand the optical behavior of alloys. Among vibrational properties, the optical phonon frequencies are evaluated. It is important to understand the effect of a pressure on dielectric and vibtraional parameters, so the derivatives of dielectric constants and phonon frequencies with respect to the pressure are also computed. The elastic constants, bulk modulus, and cohesive energy are computed to characterize the structural strength of alloys.

## 2. Method

The bandgaps of various compositions of  $\text{Zn}_{0.5}\text{Cd}_{0.5}\text{S}_y\text{Se}_{1-y}$  II–VI semiconducting quaternary alloy are computed using the empirical pseudopotential method (EPM) applying the modified virtual crystal approximation (MVCA). The MVCA accounts for disorder effects in materials due to the alloying. One can calculate the electronic bandgaps in fair agreement with experimental values using EPM at a computational cost lower than within the *ab-initio* methods [17]. The procedures of EPM and MVCA are given elsewhere [17–20] in detail. The calculations are performed considering the zinc-blende type structure for the alloy. In this diamond-like structure, the cations and anions are bonded tetrahedrally to each other. We have taken the bandgaps computed for  $\text{Zn}_x\text{Cd}_{1-x}\text{S}_y\text{Se}_{1-y}$  quaternary alloys by Paliwal *et al.* [21]. The lattice constant for the alloy is computed using Vegard’s law [22]. The important parameters, namely, the polarity ( $\alpha_p$ ) and the covalency ( $\alpha_c$ ), are evaluated by the atomic form factors ( $V^A(3)$  and  $V^S(3)$ ) used in EPM according to Vogl’s definition [23] as:

$$\alpha_p = -\frac{V^A(3)}{V^S(3)}. \quad (1)$$

After computing the bandgap for the alloy, the static refractive index ( $n$ ) is computed by the Moss relation [24]. The static refractive index ( $n$ ) is further utilized to compute the static ( $\epsilon_0$ ) and high-frequency ( $\epsilon_\infty$ ) dielectric constants using the procedure described in [25], where the Harrison bond orbital model was applied along with the VCA to compute the static ( $\epsilon_0$ ) and high-frequency ( $\epsilon_\infty$ ) dielectric constants for some alloys.

The vibrational behavior of the alloy can be understood on the basis of phonon frequencies. The Lyddane–Sachs–Teller relation [26] relates the dielectric constants ( $\epsilon_0$  and  $\epsilon_\infty$ ) to the optical longitudinal  $\omega_{\text{LO}}(0)$  and transverse  $\omega_{\text{TO}}(0)$  phonon frequencies. Using this relation, the phonon frequencies ( $\omega_{\text{LO}}(0)$  and  $\omega_{\text{TO}}(0)$ ) can be calculated at the  $\Gamma$  point of symmetry using the procedure described by Bouarissa *et al.* [25] via the following equation:

$$\omega_{\text{TO}}^2 - \omega_{\text{LO}}^2 = \frac{4\pi e_T^2 e^2}{M \Omega_0 \epsilon_\infty}. \quad (2)$$

Here,  $e_T$  is the Born transverse charge,  $M$  is twice the reduced mass, and  $\Omega_0$  is the volume occupied by one atom in a unit cell. All these parameter are obtained by EPM calculations.

The elastic constants  $c_{ij}$  show the mechanical strength of materials under the influence of strains and stresses. For cubic zinc-blende-type structures, there are 3 independent elastic constants  $c_{11}$ ,  $c_{12}$ , and  $c_{44}$ . The constants  $c_{11}$  and  $c_{12}$  are computed by utilizing the polarity ( $\alpha_p$ ) obtained by EPM within the framework proposed by Baranowski [26] and based on Harrison bond orbital model. The constant  $c_{44}$  can be calculated by the following relation [27]:

$$c_{44} = \frac{3(c_{11} + 2c_{12})(c_{11} - c_{12})}{(7c_{11} + 2c_{12})}. \quad (3)$$

For cubic crystals, the bulk ( $B$ ) and shear ( $C$ ) moduli can be computed applying the following relations [28]:

$$B = \frac{(c_{11} + 2c_{12})}{3}, \quad (4)$$

$$C = \frac{(c_{11} - c_{12})}{2}. \quad (5)$$

The cohesive energy is the energy difference between the isolated atoms and the energy of the material. The cohesive energy is computed for the alloy using an empirical relation proposed by Verma *et al.* [29].

Table 1. Computed bandgap ( $E_g$ ), refractive index ( $n$ ), dielectric constants ( $\epsilon_0$  and  $\epsilon_\infty$ ) and optical phonon frequencies ( $\omega_{\text{TO}}(0)$  and  $\omega_{\text{LO}}(0)$ ) for  $\text{Zn}_{0.5}\text{Cd}_{0.5}\text{S}_y\text{Se}_{1-y}$  alloy

$y$	Alloy	Results	$E_g$ , eV	$n$	$\epsilon_0$	$\epsilon_\infty$	$\omega_{\text{TO}}(0)$ , THz	$\omega_{\text{LO}}(0)$ , THz
0.0	$\text{Zn}_{0.5}\text{Cd}_{0.5}\text{Se}$	This work	2.27	2.54	12.12	6.46	5.17	7.08
		Expt.	2.10 <sup>a</sup> , 2.21 <sup>b</sup>	–	–	–	–	–
		Other calc. <sup>c</sup>	0.95	3.98	–	–	–	–
		Other calc. <sup>d</sup>	2.16	2.68	–	–	–	–
		Other calc. <sup>e</sup>	1.03	2.49	6.26	–	–	–
0.1	$\text{Zn}_{0.5}\text{Cd}_{0.5}\text{S}_{0.1}\text{Se}_{0.9}$	This work	2.26	2.55	12.12	6.48	5.29	7.24
0.2	$\text{Zn}_{0.5}\text{Cd}_{0.5}\text{S}_{0.2}\text{Se}_{0.8}$		2.30	2.54	12.00	6.43	5.46	7.46
0.3	$\text{Zn}_{0.5}\text{Cd}_{0.5}\text{S}_{0.3}\text{Se}_{0.7}$		2.34	2.52	11.84	6.37	5.65	7.70
0.4	$\text{Zn}_{0.5}\text{Cd}_{0.5}\text{S}_{0.4}\text{Se}_{0.6}$		2.39	2.51	11.68	6.30	5.86	7.98
0.5	$\text{Zn}_{0.5}\text{Cd}_{0.5}\text{S}_{0.5}\text{Se}_{0.5}$		2.45	2.49	11.50	6.22	6.10	8.29
0.6	$\text{Zn}_{0.5}\text{Cd}_{0.5}\text{S}_{0.6}\text{Se}_{0.4}$		2.52	2.48	11.32	6.14	6.37	8.65
0.7	$\text{Zn}_{0.5}\text{Cd}_{0.5}\text{S}_{0.7}\text{Se}_{0.3}$		2.59	2.46	11.12	6.06	6.68	9.06
0.8	$\text{Zn}_{0.5}\text{Cd}_{0.5}\text{S}_{0.8}\text{Se}_{0.2}$		2.67	2.44	10.92	5.97	7.05	9.53
0.9	$\text{Zn}_{0.5}\text{Cd}_{0.5}\text{S}_{0.9}\text{Se}_{0.1}$		2.76	2.42	10.71	5.87	7.48	10.10
1.0	$\text{Zn}_{0.5}\text{Cd}_{0.5}\text{S}$	This work	2.86	2.40	10.47	5.76	8.01	10.80
		Expt. <sup>a</sup>	2.89	–	–	–	–	–
		Other calc. <sup>c</sup>	1.11	3.39	–	–	–	–
		Other calc. <sup>f</sup>	2.82	2.48	7.0	6.2	–	–
		Other calc. <sup>g</sup>	3.06	–	–	–	–	–

<sup>a</sup>[1], <sup>b</sup>[31], <sup>c</sup>[32], <sup>d</sup>[33], <sup>f</sup>[34], <sup>e</sup>[35], <sup>g</sup>[36].

The effect of the pressure on the dielectric and vibrational parameters is analyzed by calculating the pressure derivatives of these quantities. The pressure derivatives of  $\epsilon_0$ ,  $\epsilon_\infty$ ,  $\omega_{\text{LO}}(0)$ , and  $\omega_{\text{TO}}(0)$  are computed using the relations proposed by Davydov and Tikhonov [30] as

$$\frac{\partial \epsilon_\infty}{\partial P} = -2 \frac{(1 - 3\alpha_p^2)(\epsilon_\infty - 1)}{3B}, \quad (6)$$

$$\frac{\partial \epsilon_0}{\partial P} = (1 - \epsilon_\infty) \frac{2\alpha_p^2}{3B\alpha_c^2} \left( 3 + \frac{2\alpha_p^2}{\alpha_c^2} \right) + \left( \frac{\epsilon_0 - 1}{\epsilon_\infty - 1} \right) \frac{\partial \epsilon_\infty}{\partial P}. \quad (7)$$

$$\frac{\partial \omega_{\text{TO}}}{\partial P} = \frac{\omega_{\text{TO}}}{3B} (2 + 3\alpha_p^2), \quad (8)$$

and

$$\frac{\partial \omega_{\text{LO}}}{\partial P} = \frac{\omega_{\text{TO}}}{2\sqrt{\epsilon_\infty \epsilon_0}} \left( \frac{\partial \epsilon_0}{\partial P} - \frac{\epsilon_0}{\epsilon_\infty} \frac{\partial \epsilon_\infty}{\partial P} \right) + \sqrt{\frac{\epsilon_0}{\epsilon_\infty}} \frac{\partial \omega_{\text{TO}}}{\partial P}. \quad (9)$$

Here,  $B$  is bulk modulus,  $\alpha_p$  is the polarity, and  $\alpha_c$  is the covalency obtained by the relations given previously.

### 3. Results and Discussion

#### 3.1. Optical properties

The computed bandgaps ( $E_g$ ), refractive index ( $n$ ), dielectric constants ( $\epsilon_\infty$  and  $\epsilon_0$ ), and optical phonon frequencies ( $\omega_{\text{TO}}(0)$  and  $\omega_{\text{LO}}(0)$ ) for various compositions of  $\text{Zn}_{0.5}\text{Cd}_{0.5}\text{S}_y\text{Se}_{1-y}$  II–VI semiconducting quaternary alloy are presented in Table 1.

The table shows that our computed bandgap is close to the experimental value [1, 31] for both  $\text{Zn}_{0.5}\text{Cd}_{0.5}\text{Se}$  and  $\text{Zn}_{0.5}\text{Cd}_{0.5}\text{S}$ . For other compositions, we don't have any experimental data. The value of the bandgap varies from 2.27 to 2.86 eV with the concentration of sulfur ( $y$ ) in the  $\text{Zn}_{0.5}\text{Cd}_{0.5}\text{S}_y\text{Se}_{1-y}$  alloy. It may be noted that the experimental values of bandgaps for binary materials ZnS, ZnSe, CdS, and CdSe are 3.73, 2.72, 2.46, and 1.68 eV, respectively [1]. By comparing with the other theoretical calculations [32–36] for  $\text{Zn}_{0.5}\text{Cd}_{0.5}\text{Se}$  and  $\text{Zn}_{0.5}\text{Cd}_{0.5}\text{S}$ , we found that our results are closer to the experimental findings. For  $\text{Zn}_{0.5}\text{Cd}_{0.5}\text{Se}$ , the VCA-based calculation gives bandgap values of 0.95 eV [32] and 2.16 eV [33], and the density functional theory (DFT) calculations predict it to be

Table 2. Computed elastic constants ( $c_{11}$ ,  $c_{12}$ ,  $c_{44}$ ), bulk modulus ( $B$ ), shear modulus ( $C$ ), and cohesive energy ( $E_{\text{coh}}$ ) for  $\text{Zn}_{0.5}\text{Cd}_{0.5}\text{S}_y\text{Se}_{1-y}$  alloy

$y$	Alloy	Results	Elastic constants (GPa)			$B$ (GPa)	$C$ (GPa)	$E_{\text{coh}}$ (eV/pair)
			$c_{11}$	$c_{12}$	$c_{44}$			
0.0	$\text{Zn}_{0.5}\text{Cd}_{0.5}\text{Se}$	This work	60.83	27.35	24.15	38.51	16.74	5.22
0.1	$\text{Zn}_{0.5}\text{Cd}_{0.5}\text{S}_{0.1}\text{Se}_{0.9}$		62.28	28.00	24.73	39.43	17.14	5.28
0.2	$\text{Zn}_{0.5}\text{Cd}_{0.5}\text{S}_{0.2}\text{Se}_{0.8}$		63.77	28.66	25.32	40.36	17.55	5.33
0.3	$\text{Zn}_{0.5}\text{Cd}_{0.5}\text{S}_{0.3}\text{Se}_{0.7}$		65.29	29.34	25.92	41.32	17.97	5.39
0.4	$\text{Zn}_{0.5}\text{Cd}_{0.5}\text{S}_{0.4}\text{Se}_{0.6}$		66.84	30.03	26.54	42.30	18.41	5.45
0.5	$\text{Zn}_{0.5}\text{Cd}_{0.5}\text{S}_{0.5}\text{Se}_{0.5}$		68.44	30.74	27.18	43.31	18.85	5.51
0.6	$\text{Zn}_{0.5}\text{Cd}_{0.5}\text{S}_{0.6}\text{Se}_{0.4}$		70.08	31.47	27.83	44.34	19.30	5.57
0.7	$\text{Zn}_{0.5}\text{Cd}_{0.5}\text{S}_{0.7}\text{Se}_{0.3}$		71.75	32.22	28.50	45.40	19.77	5.63
0.8	$\text{Zn}_{0.5}\text{Cd}_{0.5}\text{S}_{0.8}\text{Se}_{0.2}$		73.47	32.99	29.19	46.48	20.24	5.69
0.9	$\text{Zn}_{0.5}\text{Cd}_{0.5}\text{S}_{0.9}\text{Se}_{0.1}$		75.23	33.77	29.89	47.59	20.73	5.75
1.0	$\text{Zn}_{0.5}\text{Cd}_{0.5}\text{S}$	77.04	34.58	30.61	48.73	21.23	5.81	

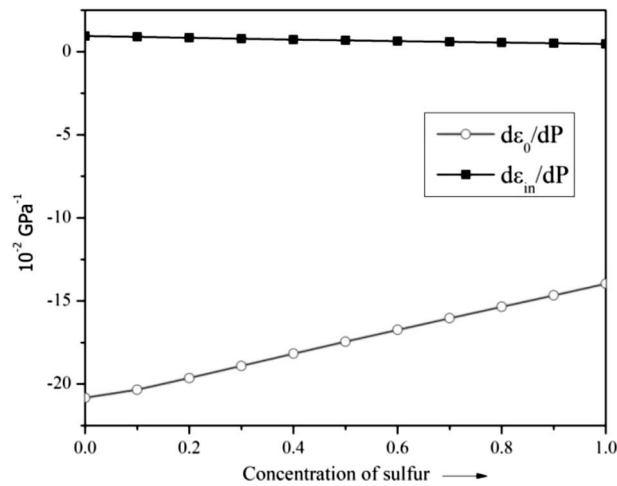


Fig. 1. Variation of the pressure derivatives of  $\varepsilon_0$  and  $\varepsilon_\infty$  with  $y$

1.03 eV showing a large deviation from the experimental value. The similar deviation from VCA calculations [32] is also found for  $\text{Zn}_{0.5}\text{Cd}_{0.5}\text{S}$ , where it gives a bandgap of 1.11 eV, while our computed value is 2.86 eV in excellent agreement with the experimental value of 2.89 eV. The DFT-computed value for  $\text{Zn}_{0.5}\text{Cd}_{0.5}\text{S}$  is 3.06 eV. These observations confirm that the MVCA approach used in this work is best suitable for finding the bandgaps of semiconducting alloys.

The refractive index slightly changes with the concentration of sulfur and decreases from 2.54 to 2.40,

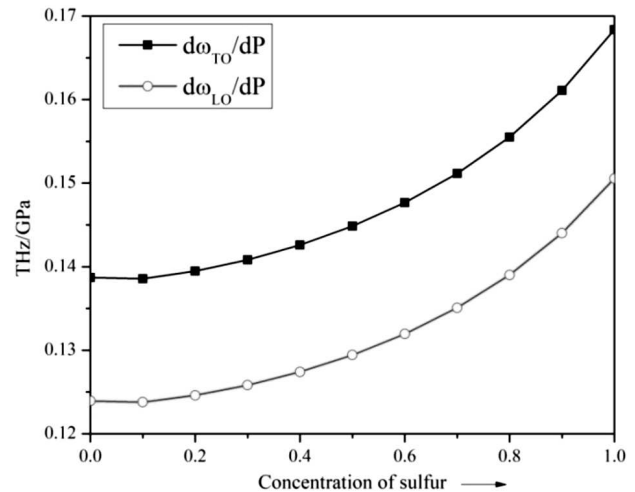


Fig. 2. Variation of the pressure derivatives of  $\varepsilon_0$  and  $\varepsilon_\infty$  with  $y$

when  $y$  changes from 0.0 to 1.0. Another feature is that both the static and high-frequency dielectric constants decrease with increasing the concentration of sulfur. The optical phonon frequencies show the opposite trend and increase with  $y$ .

The pressure derivatives of  $\varepsilon_0$ ,  $\varepsilon_\infty$ ,  $\omega_{\text{LO}}(0)$  and  $\omega_{\text{TO}}(0)$  are computed for  $\text{Zn}_{0.5}\text{Cd}_{0.5}\text{S}_y\text{Se}_{1-y}$  alloy, and their variation with the concentration of sulfur ( $y$ ) is presented in Figs. 1 and 2.

From Fig. 1, it is clear that the pressure derivative of the high-frequency dielectric constant  $d\varepsilon_\infty/dP$  (shown by black line) is positive and remains almost

constant with a variation of  $y$ . Its computed value varies between 0.5 to 1.0 (in  $10^{-2}$  GPa $^{-1}$  units). On the other hand, the pressure derivative of the static dielectric constant  $d\varepsilon_0/dP$  (shown by red line) is negative and varies between  $-20$  to  $-14$  (in  $10^{-2}$  GPa $^{-1}$  units), when  $y$  changes from 0.0 to 1.0. Its negative value shows that  $\varepsilon_0$  will decrease, when the pressure is applied. On the contrary,  $\varepsilon_\infty$  will slightly decrease. The experimental data are unavailable for the alloy, but the experimental value of  $d\varepsilon_0/dP$  for ZnSe is  $-13.6$  (in  $10^{-2}$  GPa $^{-1}$  units) [1], which is in the interval of our estimates for the alloy. The pressure derivatives of optical phonon frequencies  $\omega_{LO}(0)$  and  $\omega_{TO}(0)$  are presented in Fig. 2. Both  $d\omega_{LO}/dP$  and  $d\omega_{TO}/dP$  are positive, which indicates that the phonon frequencies increase, when the pressure is applied. In addition, both  $d\omega_{LO}/dP$  and  $d\omega_{TO}/dP$  increase, when the concentration of sulfur is increased.

### 3.2. Structural properties

In Table 2, the elastic constants, bulk modulus, shear modulus, and the cohesive energy for various compositions of Zn $_{0.5}$ Cd $_{0.5}$ S $_y$ Se $_{1-y}$  alloy is presented.

From the table, it is clear that all the structural parameters increase with the concentration of sulfur. This may be due to a small size of sulfur and its more ionic character. So, the mixing of sulfur in Zn $_{0.5}$ Cd $_{0.5}$ Se alloy increases its mechanical strength. The bulk modulus lies between 38 and 48 GPa for the alloy, while the experimental value of bulk modulus for cubic ZnS is 77 GPa [1]. So, the alloy is softer than a binary material. There are no experimental data available to compare with our estimated values for the alloy.

## 4. Results and Discussion

The optical, vibrational, and structural properties of 10 compositions of Zn $_{0.5}$ Cd $_{0.5}$ S $_y$ Se $_{1-y}$  II–VI semiconducting quaternary alloy are computed using EPM implementing the disorder effects via MVCA. The computed bandgaps are direct in nature and in better agreement with the experimental values, than the other theoretically obtained values by applying VCA and DFT approaches. This suggests that the MVCA approach is best to evaluate the bandgaps of semiconducting alloys. It has been observed that the static and high-frequency dielectric constants decrease, as the optical phonon frequencies increase,

when the sulfur concentration ( $y$ ) is increased in Zn $_{0.5}$ Cd $_{0.5}$ S $_y$ Se $_{1-y}$ . The refractive index slightly decreases with  $y$ . The computed pressure derivatives of the high-frequency dielectric constant ( $\varepsilon_\infty$ ) and static dielectric constant ( $\varepsilon_0$ ) are positive and negative, respectively. Thus, the former  $\varepsilon_\infty$  increases, while  $\varepsilon_0$  decreases on applying the pressure. The computed structural parameters such as the elastic constants, bulk modulus, shear modulus, and cohesive energy increase with the concentration of sulfur.

1. S. Adachi. *Properties of Semiconductor alloys Group IV, III–V and II–VI Semiconductors* (John Wiley & Sons, 2009) [ISBN:9780470090329].
2. S. Ikhmayies. *Introduction to II–VI Compounds. In Advances in the II–VI Compounds Suitable for Solar Cell Applications* Edited by S. Ikhmayies (Research Signpost, 2002) [ISBN: 978-81-308-0533-7].
3. K. Kishino I. Nomura. II–VI semiconductors on InP for green-yellow emitters. *IEEE J. Selected Topics in Quantum Electronics* **8**, 773 (2002).
4. R.L. Gunshor, A.V. Nurmikko. *II–VI Blue/Green Light Emitters: Device Physics and Epitaxial Growth: Semiconductors and Semimetals* (Academic Press, 1997) [ISBN: 978-0124014503].
5. P. Roblin, H. Rohdin. *High-Speed Heterostructure Devices.* (Cambridge University Press, 2002) [ISBN: 9780511754593].
6. C.-H. Moon, S.-H. Wei, Y.Z. Zhu, G.D. Chen. Band-gap bowing coefficients in large size-mismatched II–VI alloys: first-principles calculations. *Phys. Rev. B* **74**, 233202 (2006).
7. M.C. Tamargo. *II–VI Semiconductor Materials and Their Applications (Optoelectronic Properties of Semiconductors and Superlattice)* (Taylor and Francis, 2002) [ISBN: 9781560329145].
8. K. Godo, M.W. Cho, J. H. Chang, Y. Yamazaki, T. Yao, M.Y. Shen, T. Goto. Composition dependence of the energy gap of Zn $_{1-x-y}$ Mg $_x$ Be $_y$ Se quaternary alloys nearly lattice matched to GaAs. *Appl. Phys. Lett.* **79**, 4168 (2001).
9. H. Okuyama, Y. Kishita, A. Ishibashi. Quaternary alloy Zn $_{1-x}$ Mg $_x$ S $_y$ Se $_{1-y}$ . *Phys. Rev. B* **57**, 2257 (1998).
10. W.O. Charles, Y. Yao, K.J. Franz, Q. Zhang, A. Shen, C. Gmachl, M.C. Tamargo. Growth of Zn $_x$ Cd $_{(1-x)}$ Se/Zn $_x$ Cd $_y$ Mg $_{(1-x-y)}$ Se–InP quantum cascade structures for emission in the 3–5  $\mu$ m range. *J. Vac. Sci. Technol. B* **28**, C3G24 (2010).
11. Y.D. Kim, M.V. Klein, S.F. Ren, Y.C. Chang, H. Luo, N. Samarth, J.K. Furdyna. Optical properties of zincblende CdSe and Zn $_x$ Cd $_{1-x}$ Se films grown on GaAs. *Phys. Rev. B* **49**, 7262 (1994).
12. R. Venugopal, P.-I. Lin, Y.-T. Chen. Photoluminescence and Raman scattering from catalytically grown

- Zn<sub>x</sub>Cd<sub>1-x</sub>Se alloy nanowires. *J. Phys. Chem. B* **110**, 11691 (2006).
13. A. Pan, H. Yang, R. Yu, B. Zou. Fabrication and photoluminescence of high-quality ternary CdSSe nanowires and nanoribbons. *Nanotechnology* **17**, 1083 (2006).
  14. T.M. Razykov, S.Zh. Karazhanov, A.Yu. Leiderman, N.F. Khusainova, K. Kouchkarov. Effect of the grain boundaries on the conductivity and current transport in II–VI films. *Solar Energy Materials & Solar Cells* **90**, 2255 (2006).
  15. S. Fujita, S. Hayashi, M. Funato, T. Yoshie, S. Fujita. Properties of Zn<sub>1-x</sub>Cd<sub>x</sub>S ternary and Zn<sub>1-x</sub>Cd<sub>x</sub>S<sub>1-y</sub>Se<sub>y</sub> quaternary thin films on GaAs grown by OMVPE. *J. Cryst. Growth* **107**, 674 (1991).
  16. Y. Feng, K.L. Teo, M.F. Li, H.C. Poon, C.K. Ong, J.B. Xia. Empirical pseudopotential band-structure calculation for Zn<sub>1-x</sub>Cd<sub>x</sub>S<sub>y</sub>Se<sub>1-y</sub> quaternary alloy. *J. Appl. Phys.* **74**, 3948 (1993).
  17. M.L. Cohen, J.R. Chelikowsky. *Electronic Structure and Optical Properties of Semiconductors* (Springer-Verlag, 1988) [ISBN: 9783540513919].
  18. A. Bechiri, F. Benmakhlouf, N. Bouarissa. Band structure of II–V ternary semiconductor alloys beyond the VCA. *Mat. Chem. Phys.* **77**, 507 (2002).
  19. M.L. Cohen. The theory of real materials. *Annu. Rev. Mater. Sci.* **30**, 1 (2000).
  20. C.B. Swarnkar, R.K. Pandya, U. Paliwal, N.N. Patel, K.B. Joshi. Study of charge density, density of states and electron momentum density of ZnS<sub>x</sub>Se<sub>1-x</sub> semiconductor alloy. *Chalco. Lett.* **6**, 137 (2009)
  21. U. Paliwal, R.K. Kothari, K.B. Joshi. Electronic and structural properties of Zn<sub>x</sub>Cd<sub>1-x</sub>S<sub>y</sub>Se<sub>1-y</sub> alloys lattice matched to GaAs and InP: An EPM study. *Superlatt. Microstruct.* **51**, 635 (2012).
  22. L. Vegard. Die konstitution der mischkristalle und die Raumfüllung der atome. *Z. Physik.* **5**, 17 (1921).
  23. P. Vogl. Dynamical effective charges in semiconductors: A pseudopotential approach. *J. Phys. C: Solid State Physics* **1**, 251 (1978).
  24. T.S. Moss. A relationship between the refractive index and the infra-red threshold of sensitivity for photoconductors. *Proc. Phys. Soc. London B* **63**, 167 (1950).
  25. N. Bouarissa, S. Bougouffa, A. Kamli. Energy gap and optical phonon frequencies in InP<sub>1-x</sub>Sb<sub>x</sub>. *Semicond. Sci. Technol.* **20**, 265 (2005).
  26. J.M. Baranowski. Bond lengths, force constants and local impurity distortions in semiconductors. *J. Phys. C* **17**, 6287 (1984).
  27. W.A. Harrison. *Electronic Structure and the Properties of Solids: The Physics of the Chemical Bond* (Dover Publications, 1989) [ISBN: 9780486660219].
  28. M. Levinshtein, S. Rumyantsev, M. Shur. *Handbook Series on Semiconductor Parameters. Vol 2* (World Scientific, 1999) [ISBN: 9789810214203].
  29. A.S. Verma, B.K. Sarkar, V.K. Jindal. Cohesive energy of zincblende (A<sup>III</sup>B<sup>V</sup> and A<sup>II</sup>B<sup>VI</sup>) structured solids. *Pramana–J. Phys* **74**, 851 (2010).
  30. S.Yu. Davydov, S.K. Tikhonov. Elastic constants and phonon frequencies of wide-gap semiconductors. *Semiconductors* **30**, 447 (1996).
  31. M.J.S.P. Brasil, M.C. Tamargo, R.E. Nahory, H.L. Gilchrist, R.J. Martin. Zn<sub>1-y</sub>Cd<sub>y</sub>Se<sub>1-x</sub>Te<sub>x</sub> quaternary wide band-gap alloys: Molecular beam epitaxial growth and optical properties. *Appl. Phys. Lett.* **59**, 1206 (1991).
  32. K. Benchikh, H. Abid, M. Benchehima. Electronic and optical properties of ternary alloys Zn<sub>x</sub>Cd<sub>1-x</sub>S, Zn<sub>x</sub>Cd<sub>1-x</sub>Se, ZnS<sub>x</sub>Se<sub>1-x</sub>, Mg<sub>x</sub>Zn<sub>1-x</sub>Se. *Mater. Sci.-Poland* **35**, 32 (2017).
  33. N. Benosman, N. Amrane, H. Aourag. Calculation of electronic and optical properties of zinc-blende Zn<sub>x</sub>Cd<sub>1-x</sub>Se. *Physica B* **275**, 316 (2000).
  34. H. Algarni, N. Bouarissa, M.A. Khan, O.A. Al-Hagan, T.F. Alhuwaymel. Optical constants and exciton properties of Zn<sub>x</sub>Cd<sub>1-x</sub>S. *Optik* **193**, 163022 (2019).
  35. N. Korozlu, K. Colakoglu, E. Deligoz, Y.O. Ciftci. The structural, electronic and optical properties of Cd<sub>x</sub>Zn<sub>1-x</sub>Se ternary alloys. *Optics Communications* **284**, 1863 (2011).
  36. I. Bziz, El H. Atmani, N. Fazouan, M. Aazi. First-principles calculations of structural, electronic and optical properties of CdTe<sub>x</sub>S<sub>1-x</sub> and Cd<sub>1-x</sub>Zn<sub>x</sub>S ternary alloys. *Surfaces and Interfaces* **24**, 101126 (2021).

Received 18.01.23

Р.К. Джаскал, М.Д. Шарма, Ю. Паливал

ТЕОРЕТИЧНА ОЦІНКА  
ОПТИЧНИХ, ВІБРАЦІЙНИХ  
ТА СТРУКТУРНИХ ВЛАСТИВОСТЕЙ  
ЧОТИРИКОМПОНЕНТНОГО СПЛАВУ  
З ЕЛЕМЕНТІВ ІІ ТА VI ГРУП Zn<sub>0,5</sub>Cd<sub>0,5</sub>S<sub>y</sub>Se<sub>1-y</sub>

Зроблено теоретичну оцінку оптичних, вібраційних та структурних властивостей чотирикомпонентного напівпровідникового сплаву з елементів ІІ та VI груп Zn<sub>0,5</sub>Cd<sub>0,5</sub>S<sub>y</sub>Se<sub>1-y</sub> для 0 < y < 1, всього для 10 варіантів композицій. Розраховано показник заломлення, коефіцієнти пружності, об'ємний модуль пружності та частоти коливань з використанням вихідних параметрів методу емпіричного псевдопотенціалу. Знайдено щільності енергетичного спектра і змодельовано ефекти сплавлення у модифікованому наближенні віртуального кристала. Розраховано статичний показник заломлення, діелектричні константи у статичному випадку та для високих частот, обчислено частоти оптичних фононів, коефіцієнти пружності, об'ємний модуль пружності та енергію когезії для 10 композицій сплаву. Результати порівнюються з іншими теоретичними і експериментальними даними.

*Ключові слова:* чотирикомпонентні сплави з елементів ІІ та VI груп, метод емпіричного псевдопотенціалу, коефіцієнти пружності.